Article

Multi-Step Microfluidic Polymerization Reactions Conducted in Droplets: The Internal Trigger Approach

Wei Li, Hung H. Pham, Zhihong Nie, Brendan MacDonald, Axel Gu#enther, and Eugenia Kumacheva

J. Am. Chem. Soc., **2008**, 130 (30), 9935-9941 • DOI: 10.1021/ja8029174 • Publication Date (Web): 02 July 2008

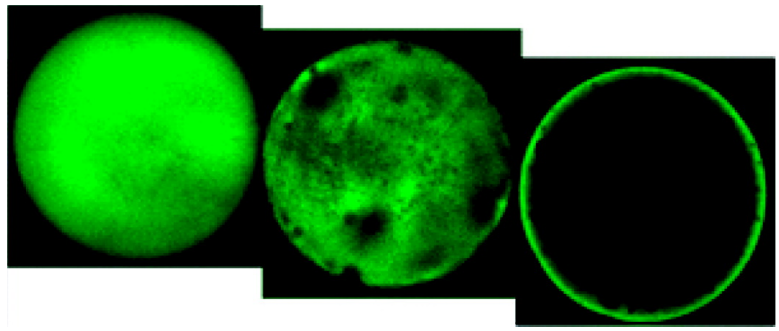

J|A|C|S
ARTICLES

Published on Web 07/02/2008

Multi-Step Microfluidic Polymerization Reactions Conducted in Droplets: The Internal Trigger Approach

Wei Li,[†] Hung H. Pham,[†] Zhihong Nie,[†] Brendan MacDonald,[‡] Axel Güenther,[‡] and Eugenia Kumacheva*,[†]

Department of Chemistry, University of Toronto, Toronto, Ontario M5S 3H6, Canada, and Department of Mechanical & Industrial Engineering, University of Toronto, 5 King's College Road, Toronto, Ontario M5S 3G8, Canada

Received April 20, 2008; E-mail: ekumache@chem.utoronto.ca

Abstract: We report the application of the "internal trigger" approach to multistep microfluidic polymerization reactions conducted in droplets, namely, polyaddition and polycondensation. We hypothesized and experimentally established that heat generated in an exothermic free radical polymerization of an acrylate monomer (Reaction 1) triggers the polycondensation of the urethane oligomer (Reaction 2). Completion of two microfluidic polymerization reactions led to the continuous synthesis of polymer particles with an interpenetrating polymer network (IPN) structure. Use of this microfluidic synthesis allowed us (i) to conduct efficient screening of the compositions of the monomer mixtures; (ii) to achieve control of the stoichiometric ratios of reactants in Reaction 2 by varying the flow rates of liquids; (iii) to reach control over the morphology of the resulting particles; and (iv) to produce polymer particles with a narrow size distribution and a predetermined size.

Introduction

Microfluidic synthesis is characterized by the ability to control the location and time of chemical reactions by using the distance-to-time transformation.[1] This feature is particularly important for multistep chemical reactions: the relation $t = d/U$, where t is the elapsed time of the reaction, d is the distance traveled through a microchannel, and U is the flow velocity, allows microfluidic synthesis to be conducted in a highly controllable manner. Recently, several research groups have reported successful multistep microfluidic syntheses of a range of organic and inorganic compounds,[2,3] in which sequential reactions were elicited by introducing into the microchannels reagents required in the corresponding step.

Microfluidic synthesis compartmentalized within droplets offers several attractive features, such as suppressed dispersion, accurate control of surface chemistry at the liquid−liquid interface, efficient mixing, and the ability of high-throughput screening of reaction conditions.[4] Single-step reactions performed in droplets include nitration of benzene, fluorination of aromatics, bromination of alkenes, and reactions in which the product precipitates in the droplet phase, e.g., the synthesis of indigo or 4-chloro-*N*-methylbenzamide.[5] Single-step reactions conducted in droplets have also been used for the continuous microfluidic synthesis of polymer and inorganic particles.[6,7]

Multistep microfluidic synthesis within droplets can be conducted in several ways. In the first approach, after allowing the reagents compartmentalized within a droplet to react for a certain time, the reagent(s) required in the successive reaction is introduced in the droplet by controlled coalescence with another droplet,[1e,8] direct addition of reagents into the droplets through a side channel,[5e,9] or by diffusion from the continuous phase.[10]

In an alternative approach to multistep synthesis, droplets flowing through the microchannels may contain all of the reactants required for the multistep reactions; however, each reaction is selectively initiated by using external or internal

[†] Department of Chemistry, University of Toronto.
[‡] Department of Mechanical & Industrial Engineering, University of Toronto.

(1) (a) De Mello, A.; Wootton, R. *Lab Chip* **2002**, *2*, 7n–13n. (b) De Mello, A. *Nature* **2006**, *442*, 394–402. (c) Jensen, K. F. *Chem. Eng. Sci.* **2001**, *56*, 293–303. (d) Jähnisch, K.; Hessel, V.; Löwe, H.; Baerns, M. *Angew. Chem., Int. Ed.* **2004**, *43*, 406–446. (e) Song, H.; Tice, J. D.; Ismagilov, R. F. *Angew. Chem., Int. Ed.* **2003**, *42*, 768–772.
(2) (a) Jas, G.; Kirschning, A. *Chem. Eur. J.* **2003**, *9*, 5708–5723. (b) Lee, C. C.; et al. *Science* **2005**, *310*, 1793–1796. (c) Sahoo, H. R.; Kralj, J. G.; Jensen, K. F. *Angew. Chem., Int. Ed.* **2007**, *46*, 5704–5708. (d) Uozumi, Y.; Yamada, Y. M. A.; Beppu, T.; Fukuyama, N.; Ueno, M.; Kitamori, T. *J. Am. Chem. Soc.* **2006**, *128*, 15994–15995. (e) Kobayashi, J.; Mori, Y.; Okamoto, K.; Akiyama, R.; Ueno, M.; Kitamori, T.; Kobayashi, S. *Science* **2004**, *304*, 1305–1308.
(3) (a) Wagner, J.; Köhler, J. M. *Nano Lett.* **2005**, *4*, 685–691. (b) Inoue, T.; Schmidt, M. A.; Jensen, K. F. *Ind. Eng. Chem. Res.* **2007**, *46*, 1153–1160.
(4) (a) Song, H.; Bringer, M. R.; Tice, J. D.; Gerdts, C. J.; Ismagilov, R. F. *Appl. Phys. Lett.* **2003**, *83*, 664–4666. (b) Song, H.; Chen, D. L.; Ismagilov, R. F. *Angew. Chem. Int. Ed* **2006**, *45*, 7336–7356. (c) Zheng, B.; Ismagilov, R. F. *Angew. Chem., Int. Ed.* **2005**, *44*, 2520–2523. (d) Atencia, J.; Beebe, D. J. *Nature* **2005**, *437*, 648–655. (e) Okushima, S.; Nisisako, T.; Torii, T.; Higuchi, T. *Langmuir* **2004**, *20*, 9905–9908. (f) Li, W.; Nie, Z. H.; Zhang, H.; Paquet, C.; Seo, M.; Garstecki, P.; Kumacheva, E. *Langmuir* **2007**, *23*, 8010–8014. (g) Barnes, S. E.; Cygan, Z. T.; Yates, J. K.; Beers, K. L.; Amis, E. J. *Analyst* **2006**, *131*, 1027–1033.
(5) (a) Burns, J. R.; Ramshaw, C. *Chem. Eng. Commum.* **2002**, *189*, 1611–1628. (b) De Mas, N.; Gunther, A.; Schmidt, M. A.; Jensen, K. F. *Ind. Eng. Chem. Res.* **2003**, *42*, 698–710. (c) Cygan, Z. T.; Cabral, J. T.; Beers, K. L.; Amis, E. J. *Langmuir* **2005**, *21*, 3629–3634. (d) Burns, J. R.; Ramshaw, C. *Lab Chip* **2001**, *1*, 10–15. (e) Poe, S. L.; Cummings, M. A.; Haaf, M. R.; McQuade, D. T. *Angew. Chem., Int. Ed.* **2006**, *45*, 1544–1548.

triggers. Photoirradiation at several distinct wavelengths, local changes in temperature, or application of an electric field can serve as possible external triggers. Internal triggers are created in situ when the preceding reaction yields a product that acts as a reactant in the subsequent reaction, or when the preceding reaction generates energy, which activates the successive reaction.

In the present paper, we report the application of the "internal trigger" approach to multistep microfluidic polymerization reactions compartmentalized in droplets, namely, the reactions of polyaddition and polycondensation. We hypothesized and experimentally established that heat generated in the exothermic free radical polymerization of the acrylate monomer (Reaction 1) triggers polycondensation of the urethane oligomer (Reaction 2). Completion of two polymerization reactions under optimized conditions led to the continuous microfluidic synthesis of polymer particles with an interpenetrating polymer network (IPN) structure. IPN polymers find a broad range of applications as foams, membranes, coatings and as materials for sound and vibration damping. Current methods used for producing micrometer-size IPN particles lack control over particle size and morphology. The use of the microfluidic synthesis allowed us to optimize the composition of the reaction mixture by varying the flow rates of liquid reactants and to achieve control over the dimensions and morphology of the resultant polymer particles.

Proposed Approach. We selected photoinitiated free radical polymerization of tri(propylene glycol) diacrylate (TPGDA) as Reaction 1 and condensation of poly(propylene glycol) tolylene 2,4-diisocyanate (PU-pre) with diethanolamine (DEA) as Reaction 2 (Scheme 1). Photoinitiated free radical polymerization reactions of acrylates are exothermic and fast: the enthalpies of these reactions are in the range from 55 to 86 kJ/mol[11] and reaction rate constants are on the order of $\sim 10^2 - 10^4$ $Lmol^{-1}s^{-1}$.[12] In contrast, the condensation between the −NCO and −OH groups at room temperature occurs at low rate, which, however can be increased at elevated temperatures (the activation energy of these reactions is on the order of $\sim 10^2$ kJ/mol).[13]

Figure 1 illustrates the approach to a two-step microfluidic polymerization. A droplet mixture of TPGDA and a photoinitiator 2-diethoxyacetophenone (DEAP) (reagents for Reaction 1) and PU-pre, DEA, and a catalyst dibutyltin dilaurate (DBTDL) (reagents for Reaction 2) is exposed to UV-irradiation. Photoinitiated free radical polymerization yields a polyTPGDA network[6c] and generates heat which activates the polycondensation of PU-pre. When both polymerization reactions proceed to high conversion and macroscopic phase separation of the polymers is suppressed, the two-step synthesis yields polyTPGDA-polyurethane particles with an IPN structure.

In the approach illustrated in Figure 1, high conversion of PU-pre within the time of residence of the droplets in the microfluidic reactor is achieved by controlling the amount of heat generated in Reaction 1 and accounting for the amount of heat dissipated in the continuous phase. Control of the amount of heat produced in Reaction 1 is accomplished by varying the relative fraction of the reagents consumed in Reaction 1 and is realized by changing the flow rates of the monomers supplied to the microfluidic reactor. The stoichiometric ratios between the −NCO groups of PU-pre and −OH groups of DEA are also ensured by controlling the flow rates of the corresponding liquid monomers.

The droplets of the reaction mixture are dispersed in the aqueous phase comprising a polymeric stabilizer poly(vinyl alcohol) (PVA). The reactions of −NCO groups with water and/or PVA can, in principle, affect the stoichiometry between the −NCO and −OH groups and, therefore, can lead to a decrease in conversion of PU-pre;[13] however, we assumed that these side reactions are limited to the droplet−water interface and because of the short reaction times and relatively large dimensions of the droplets would not significantly affect polymerization occurring in the droplet.

Experimental Design

Figure 2 shows a schematic of the continuous microfluidic reactor used in the present work. The mixtures of the monomers were introduced into the mixing compartment via three inlets. The reagents for Reaction 2 included PU-pre, a cross-linker DEA, and a catalyst DBTDL. To avoid the reaction between the −NCO and −OH groups of PU-pre and DEA prior to their introduction into the reactor, the PU-pre/DEA and PU-pre/DBTDL mixtures were supplied through two separate side inlets: *inlet 1* and *inlet 3*, respectively. The reagents for free radical polymerization—the mixture of TPGDA and DEAP—were introduced in the central *inlet 2*.

The weight ratios of the reagents for Reactions 1 and 2 were controlled by changing the ratios of flow rates, Q_1, Q_2, and Q_3

(6) (a) Nisisako, T.; Torii, T.; Higuchi, T. *Chem. Eng. J.* **2004**, *101*, 23–29. (b) Jeong, W. J.; Kim, J. Y.; Choo, J.; Lee, E. K.; Han, C. S.; Beebe, D. J.; Seong, G. H.; Lee, S. H. *Langmuir* **2005**, *21*, 3738–3741. (c) Xu, S.; Nie, Z.; Seo, M.; Lewis, P. C.; Kumacheva, E.; Stone, H. A.; Garstecki, P.; Weibel, D. B.; Gitlin, I.; Whitesides, G. M. *Angew. Chem., Int. Ed.* **2005**, *44*, 724–728. (d) Dendukuri, D.; Tsoi, K.; Hatton, T. A.; Doyle, P. S. *Langmuir* **2005**, *21*, 2113–2116. (e) Nie, Z. H.; Li, W.; Seo, M.; Xu, S. Q.; Kumacheva, E. *J. Am. Chem. Soc.* **2006**, *128*, 9408–9412. (f) Nie, Z. H.; Xu, S.; Seo, M.; Lewis, P. C.; Kumacheva, E. *J. Am. Chem. Soc.* **2005**, *127*, 8058–8063. (g) Seo, M.; Xu, S.; Nie, Z. H.; Lewis, P. C.; Graham, R.; Mok, M.; Kumacheva, E. *Langmuir* **2005**, *21*, 4773–4775. (h) Lewis, P. C.; Graham, R.; Xu, S.; Nie, Z. H.; Seo, M.; Kumacheva, E. *Macromolecules* **2005**, *38*, 4536–4538.

(7) (a) Chan, E. M.; Alivisatos, A. P.; Mathies, R. A. *J. Am. Chem. Soc.* **2005**, *127*, 13854–13861. (b) Nakamura, H.; Yamaguchi, Y.; Miyazaki, M.; Maeda, H.; Uehara, M.; Mulvaney, P. *Chem. Comm.* **2002**, *23*, 2844–2845. (c) Khan, S. A.; Gunther, A.; Schmidt, M. A.; Jensen, K. F. *Langmuir* **2004**, *20*, 8604–8611.

(8) (a) Link, D. R.; Grasland-Mongrain, E.; Duri, A.; Sarrazin, F,.; Cheng, Z. D.; Cristobal, G.; Marquez, M.; Weitz, D. A. *Angew. Chem., Int. Ed.* **2006**, *45*, 2556–2560. (b) Li, L.; Boedicker, J. Q.; Ismagilov, R. F. *Anal. Chem.* **2007**, *79*, 2756–2761. (c) Gerdts, C. J.; Sharoyan, D. E.; Ismagilov, R. F. *J. Am. Chem. Soc.* **2004**, *126*, 6327–6331. (d) Sugiura, S.; Oda, T.; Izumida, Y.; Aoyagi, Y.; Satake, M.; Ochiai, A.; Ohkohchi, N.; Nakajima, M. *Biomaterials* **2005**, *26*, 3327–3331.

(9) (a) Shestopalov, I. A.; Tice, J. D.; Ismagilov, R. F. *Lab Chip* **2004**, *4*, 316–321. (b) Song, H.; Li, W. H.; Munson, M. S.; Van, Ha., T. G.; Ismagilov, R. F. *Anal. Chem.* **2006**, *78*, 4839–4849.

(10) (a) Zhang, H.; Tumarkin, E.; Peerani, R.; Nie, Z. H.; Sullan, R. M. A.; Walker, G. C.; Kumacheva, E. *J. Am. Chem. Soc.* **2006**, *128*, 12205–12210. (b) Zhang, H.; Tumarkin, E.; Sullan, R. M. A.; Walker, G. C.; Kumacheva, E. *Macromol. Rapid Commun.* **2007**, *28*, 527–538. (c) Shepherd, R. F.; Conrad, J. C.; Rhodes, S. K.; Link, D. R.; Marquez, M.; Weitz, D. A.; Lewis, J. A. *Langmuir* **2006**, *22*, 8618–8622.

(11) (a) Miyazaki, K.; Horibe, T. J. *J. Biomed. Mater. Res.* **1988**, *22*, 1011–1022. (b) Anseth, K. S.; Wang, C. M.; Bowman, C. N. *Macromolecules* **1994**, *27*, 650–655.

(12) Moore, J. E. *Chemistry and Properties of Crosslinked Polymers*; Labana, S. S., Ed.; Academic: New York, 1977; p 535. (d) Kaczmarek, H.;; Decker, C. *J. Appl. Polym. Sci.* **1994**, *54*, 2147–2156.

(13) (a) Chang, M. C.; Chen, S. A. *J. Polym. Sci., Part A: Polym. Chem.* **1987**, *25*, 2534–2539. (b) Kim, S. C.; Sperling, L. H. *IPNs Around The World: Science and Engineering*; John Wiley & Sons: Chichester, England, 1997. (c) Mezhikovskii, S. M. *Physico-Chemical Principles for Process of Oligomeric Blends*; Gordon and Breach Science Publishers: The Netherlands, 1998. (d) Smirnova, N. N.; Kandeev, K. V.; Markin, A. V.; Bykova, T. A.; Kulagina, T. G.; Fainleib, A. M. *Thermochim. Acta* **2006**, *445*, 7–18.

Scheme 1. Polyaddition of TPGDA (Reaction 1) and Polycondensation of PU-Pre (Reaction 2)[a]

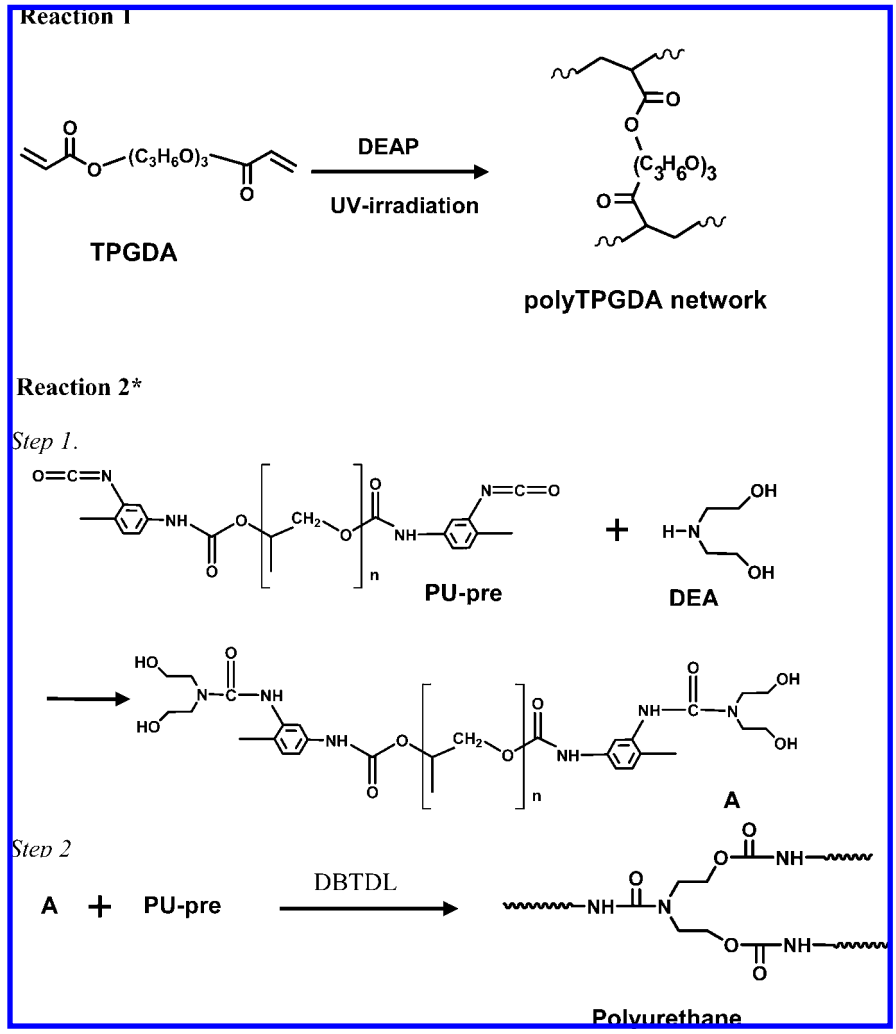

[a] In Step 1 of Reaction 2, the −NCO groups of PU-pre rapidly react with the −NH groups of DEA (no catalyst is required for this setp). In Step 2, the reaction between the −OH groups of DEA and the −NCO groups of PU-pre occurs at low rate and requires a catalyst dibutyltin dilaurate (DBTDL). We proposed that the heat generated in Reaction 1 will accelerate the second step of Reaction 2.

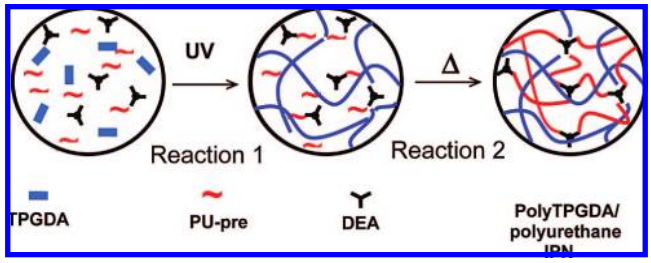

Figure 1. Schematics of multistep polyaddition and polycondensation reactions conducted in a droplet comprising a mixture of TPGDA monomer, PU-pre, and PU-cross-linker DEA. The molecules of the photoinitiator and catalyst are not shown in order to simplify the schematics.

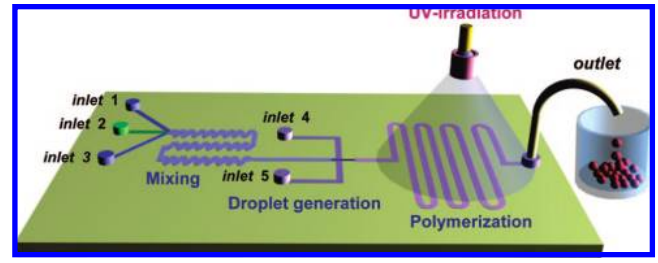

Figure 2. Schematic of the microfludic reactor. A mixture of PU-pre/DEA at weight ratio 96/4, respectively, is supplied to *inlet 1*; a mixture of TPGDA/DEAP at weight ratio 96/4, respectively, is supplied in *inlet 2*; a mixture of PU-pre/DBTDL at weight ratio 98/2, respectively, is supplied in *inlet 3*, and a 3 wt% aqueous solution of poly(vinyl alcohol) (PVA) is supplied to *inlets 4* and *5*. After mixing in the mixing zone, the weight ratio of PU-pre/DEA/DBTDL is 96/3/1. Droplets of the monomer mixture move to the polymerization zone where they are exposed to UV-irradiation. The lengths of the serpentine channels in the mixing zone and the polymerization zone are 75 and 500 mm, respectively.

of the liquid reactants supplied to *inlets 1, 2*, and *3*, respectively. The stochiometric ratio between the reactants in Reaction 2 (corresponding to the weight ratio PU-pre/DEA/DBTDL of 96:3:1) was controlled by setting the corresponding flow rates of the liquid mixtures introduced in *inlets 1* and *3* at $Q_1 = Q_3$.

After mixing the reagents in the serpentine channel (designated as "Mixing" in Figure 2) the reaction mixture was forced into the droplet generator zone, in which a 3 wt% aqueous solution of PVA was introduced into the side channels via *inlets 4* and *5*. The monomer mixture and the aqueous solution were forced into a narrow orifice in which a monomer thread periodically broke up and released droplets. The droplets moved to the "Polymerization" zone (Figure 2) where they were exposed to UV-irradiation (Dr. Hönle UVA Print 40C, F-lamp, 400 W, λ= 330−380 nm) for the

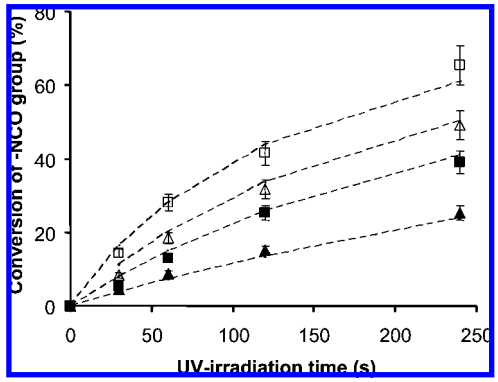

Figure 3. Experimentally determined conversion of the isocyanate groups of PU-pre in the particles synthesized from the TPGDA/PU-pre mixtures at α of 0.14 (▲), 0.42 (■), 0.98 (△), and 2.29 (□), plotted as a function of UV-irradiation time. Dashed lines show that the best fit for the estimated conversion of the −NCO groups (see Supporting Information) was achieved at $f = 0.16$ (▲), 0.12 (■), 0.095 (△), and 0.09 (□).

time intervals varying from 30 s to 4 min. The resulting particles were collected at the outlet of the reactor.

Results and Discussion

Testing the Hypothesis. In the approach illustrated in Figure 1, in order to achieve high conversion in Reaction 2 within a relatively short interval of time, Reaction 1 must produce a sufficient amount of heat. Thus, the weight ratio, α, between the amounts of reactants consumed in Reaction 1 and Reaction 2 (later in the text referred to as the TPGDA/PU-pre mixture) becomes a critically important parameter in controlling the temperature of the droplet.

To test our hypothesis, we determined rate constants of Reaction 2 at different temperatures and calculated the value of activation energy, ΔE_a, of this reaction. Second, we established the relationship between the value of α (controlling the temperature in droplets) and conversion of the −NCO groups of PU-pre achieved within different *on-chip* UV-irradiation times of monomer droplets. We assumed that (i) the droplets have a uniform composition with an average heat capacity; (ii) the heat capacity of the monomer and polymer mixtures are equal, (iii) uniform heat transfer from the droplets to the continuous phase occurs within the time of residence of the droplets in the polymerization zone; and (iv) no temperature gradients exist within the droplets. The details of the calculations are provided in Supporting Information.

Figure 3 shows the variation in experimentally determined and estimated conversions of the −NCO groups of PU-pre for the values of α of 0.14, 0.42, 0.98, and 2.29, respectively. The dashed lines show the theoretical conversions achieved at various fractions, *f*, of heat generated in Reaction 1 and absorbed by the droplets. At low values of α, 0.14 and 0.42, less heat was produced by polymerizing a smaller amount of TPGDA, and the temperatures of the droplets were lower than those at α of 0.98 and 2.98. Smaller difference between the temperature of the droplets and the continuous phase resulted in a larger value of *f*.

In experiments, the value of α was tuned by varying the weight ratios of the reagents (determined by their flow rate ratios). Off-chip polymerization of PU-pre was quenched by liquid nitrogen. Conversion of the isocyanate groups increased with increasing value of α, due to the larger amount of heat generated in the droplets, e.g., for $\alpha = 0.14$ and $\alpha = 2.29$ conversion was 25% and 65%, respectively. We note that conversion of 65% achieved in 4 min of UV-polymerization was in the range of 60−80% typically achieved for the polymerization of polyurethane: in this range of conversions, the system reaches the gel point, at which further polymerization occurs very slowly.[13]

Table 1. Exploring Two-Step Polyaddition and Polycondensation Reactions[a,b]

system	*inlet 1* TPGDA/ PU-pre/DEAP	*inlet 3* TPGDA/ PU-pre/DBTDL	UV-exposure	conversion (polyaddition) (%)	conversion (polycondensation) (%)
S1	+	−	−	0	0
S2	+	+	−	0	∼3%
S3	−	+	+	0	∼5%
S4	+	−	+	>90%	∼2%
S5	+	+	+	>90%	∼68%

[a] UV-irradiation was conducted for 4 min. The compositions of the reaction mixtures supplied to the inlets was: *inlet 1* (62 wt% TPGDA, 30 wt% Pre-PU, 8 wt% DEAP), *inlet 2* (69.9 wt% TPGDA, 27 wt% PU-pre, 3 wt% DEA, and 0.1% HY-MA), *inlet 3* (70 wt% TPGDA, 29 wt% Pre-PU, 1 wt% DBTDL), and *inlets 4 and 5* (3 wt% aqueous solution of PVA, flow rate 0.5 mL/hr). *Inlet 2* was open for all 5 systems. The flow rates of the liquids introduced in *inlets 1−3* (when open) were 0.012 mL/hr. [b] +: "open", −: "closed".

In the second step, by showing that without the heat generated in Reaction 1, the second reaction does not precede to a significant extent within the time of microfluidic synthesis, we established that Reaction 2 is indeed triggered by Reaction 1. The results of the control microfluidic reactions (all conducted at $\alpha = 2.29$) are summarized in Table 1. By selectively opening (+) or closing (−) specific inlets, and exposing (+) or not exposing (−) the droplets to UV-irradiation, we changed the reaction conditions and the compositions of the reaction mixtures.

In system S1, in the absence of the photoinitiated polyaddition of TPGDA and the catalyst DBTDL, no notable conversion of PU-pre was measured. In system S2, conversion of the −NCO groups was ∼3%, suggesting that (i) the reaction between the −OH and −NCO groups occurred very slowly and (ii) the reaction between the isocyanate groups and water or poly(vinyl alcohol) did not play a significant role. In system S3, in the absence of photoinitiator the polymerization of TPGDA did not proceed. Low conversion of the −NCO groups of ∼5% occurred, presumably due to the weak absorption of UV-light by PDMS and the PVA solution.[14] In system S4, without the catalyst DBTDL, conversion of the −NCO groups was lower than 2%. In system S5, conversion of the −NCO groups of 68% was reached, which is typical for polycondensation of polyurethane: earlier experiments showed that at conversion of 60−80%, the system reaches gel point, at which further increase in conversion of −NCO groups occurs very slowly.[13] Thus, we conclude that in the multistep microfluidic synthesis, Reaction 2 proceeded to a significant extent, owing to the photoinitiated Reaction 1.

Mixing of Monomers. Since in the laminar flow diffusion-controlled mixing of the reagents is slow,[15] we monitored mixing of the reagents by introducing a small amount of methacrylate covalently labeled with a fluorescent Hostasol Yellow (HY-MA) in the liquid supplied to *inlet 2* (Figure 4a).

(14) (a) Jin., S. R.; Meyer, G. C. *Polymer* **1986**, *27*, 592–596. (b) Modesti, M.; Lorenzetti, A. *Eur. Polym. J.* **2001**, *37*, 949–954.
(15) (a) Hu, S. W.; Ren, X. Q.; Bachman, M.; Sims, C. E.; Li, G. P.; Allbritton, N. *Anal. Chem.* **2002**, *74*, 4117–4123. (b) Makamba, H.; Kim, J. H.; Lim, K.; Park, N.; Hahn, J. H. *Electrophoresis* **2003**, *24*, 3607–3619.

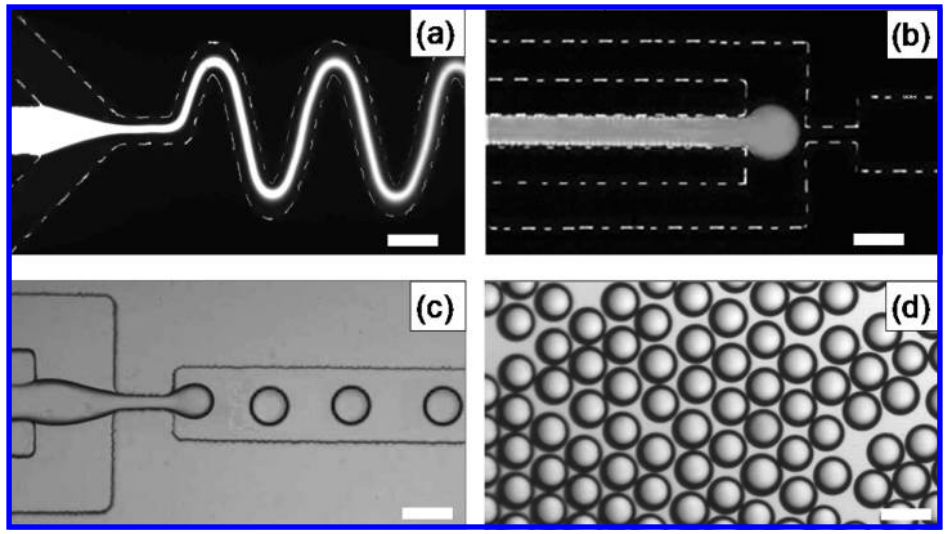

Figure 4. Fluorescence microscopy images of the mixture of monomers in the mixing zone (a) and in the central channel of the droplet generator (b). The contours of the microchannels are shown with a dashed line. The stream of the TPGDA/DEAP mixture at weight ratio 96/4, respectively, and a HY-MA is supplied to the central channel of the reactor. (c) Microfluidic emulsification of the PU-pre/TPGDA mixture at $\alpha = 0.98$. The flow rates of the PU-pre/TPGDA mixture and the continuous aqueous phase are 0.036 and 1.0 mL/h, respectively. The mean diameter of the droplets is 135 μm (CV = 1.8%). (d) Droplets of the PU-pre/TPGDA mixture collected at the outlet of the microfluidic reactor without exposure to UV-irradiation. The mean diameter of the droplets is 132 μm (CV = 2.5%). Scale bar is 200 μm.

Mixing of the reactants was favored by passing them through a serpentine channel (labeled as "Mixing" zone in Figure 2) and by flow-focusing the thread of the reagents in the orifice.[4a,16] Figure 4b shows that complete mixing of the reagents was achieved when the monomers entered the droplet generator.

Microfluidic Emulsification. The flow rate of the continuous aqueous phase was varied from 0.4 to 2.0 mL/hr and the flow rate of the TPGDA/PU-pre mixture was changed from 0.012 to 0.036 mL/h. The droplets formed in the dripping, flow-focusing, or the jetting regime.[17] The emulsification regime depended on the flow rates of the liquids and the composition of the TPGDA/PU-pre mixture. Larger droplets were produced from the mixtures at a lower α, which had a higher viscosity (see Supporting Information). The mean diameters of the droplets were in the range from 50 to 150 μm. Under optimized emulsification conditions, the polydispersity of the droplets, characterized by the coefficient of variance (CV, defined as $(\delta/D_m) \times 100\%$, where δ is the standard deviation and D_m is the mean diameter of droplet) did not exceed 3%. Figure 4c,d shows typical optical microscopy images of the emulsification of the PU-pre/TPGDA mixture at $\alpha = 0.98$ and the droplets collected at the outlet of the microfluidic reactor, respectively.

Surface Morphology and Internal Structure of Polymer Microbeads. Following 4-min UV-irradiation of the droplets of the TPGDA/PU-pre mixtures at $\alpha = 0.98$ and $\alpha = 2.29$, the polymer particles were collected at the outlet of the microfluidic reactor. Conversion of TPGDA exceeded 90%, and conversions of PU-pre were 53% and 68% for the particles obtained from the TPGDA/PU-pre mixtures at $\alpha = 0.98$ and $\alpha = 2.29$, respectively. The particles were washed with acetone and methanol to remove unreacted monomers and/or noncross-linked polymers, and characterized using optical microscopy, Scanning Electron Microscopy (SEM), and Confocal Fluorescence Microscopy (CFM).

Figure 5a,b shows representative SEM images of the surface of polymer particles obtained by the two-step microfluidic synthesis. The particles had a spherical shape and a polydispersity below 3%. The diameters of the particles were 5−10% smaller than the corresponding droplets, due to the shrinkage of the polymer upon polymerization. Because at $\alpha = 0.98$ the monomer mixture had a higher viscosity (see Supporting Information), the size of droplets and the corresponding particles generated from this mixture was slightly larger than those for the droplets and particles obtained from the TPGDA/PU-pre mixture at $\alpha = 2.29$.[7b,18] More importantly, the SEM images in Figure 5c,d show the difference between the surface morphologies of the microbeads synthesized from the monomer mixtures with different compositions. The particles synthesized from the TPGDA/PU-pre at $\alpha = 0.98$ had a smooth surface (Figure 5c), whereas the surface of particles synthesized from the TPGDA/PU-pre mixture at $\alpha = 2.29$ featured a porous structure (Figure 5d). In the latter system, a higher conversion of PU-pre was achieved, causing a decrease in the compatibility between PU-pre and TPGDA and a substantial phase separation in the polymer mixture. Phase separation visualized by extracting large cross-linked PU-rich domains with acetone, which left behind pores on the surface of particles.

Furthermore, we examined the internal structure of the microbeads using confocal fluorescence microscopy (CFM). Prior to these experiments, we verified that fluorescent HY-MA strongly partitions and copolymerizes with TPGDA. Figure 6a,b shows typical CFM images of the particles synthesized from the TPGDA/PU-pre mixtures at α of 0.98 and 2.29, respectively. In Figure 5a, a relatively uniform distribution of the dye indicated a uniform distribution of polyTPGDA and

(16) (a) Auroux, P. A.; Iossifidis, D.; Reyes, D. R.; Manz, A. *Anal. Chem.* **2002**, *74*, 2623–2636. (b) Ismagilov, R. F.; Stroock, A. D.; Kenis, P. J. A.; Whitesides, G. M.; Stone, H. A. *Appl. Phys. Lett.* **2000**, *76*, 2376–2378.

(17) (a) Stroock, A. D.; Dertinger, S. K. W.; Ajdari, A.; Mezic, I.; Stone, H. A.; Whitesides, G. M. *Science* **2002**, *295*, 647–651. (b) Tice, J. D.; Song, H.; Lyon, A. D.; Ismagilov, R. F. *Langmuir* **2003**, *19*, 9127–9133.

(18) (a) Anna, S. L.; Bontoux, N.; Stone, H. A. *Appl. Phys. Lett.* **2003**, *82*, 364–366. (b) Garstecki, P.; Stone, H. A.; Whitesides, G. M. *Phys. Rev. Let.,* **2005**, *94*, 164501/1–164501/4. (c) Christopher, G. F.; Anna, S. L. J. *Phys. D: Appl. Phys.* **2007**, *40*, R319–R336.

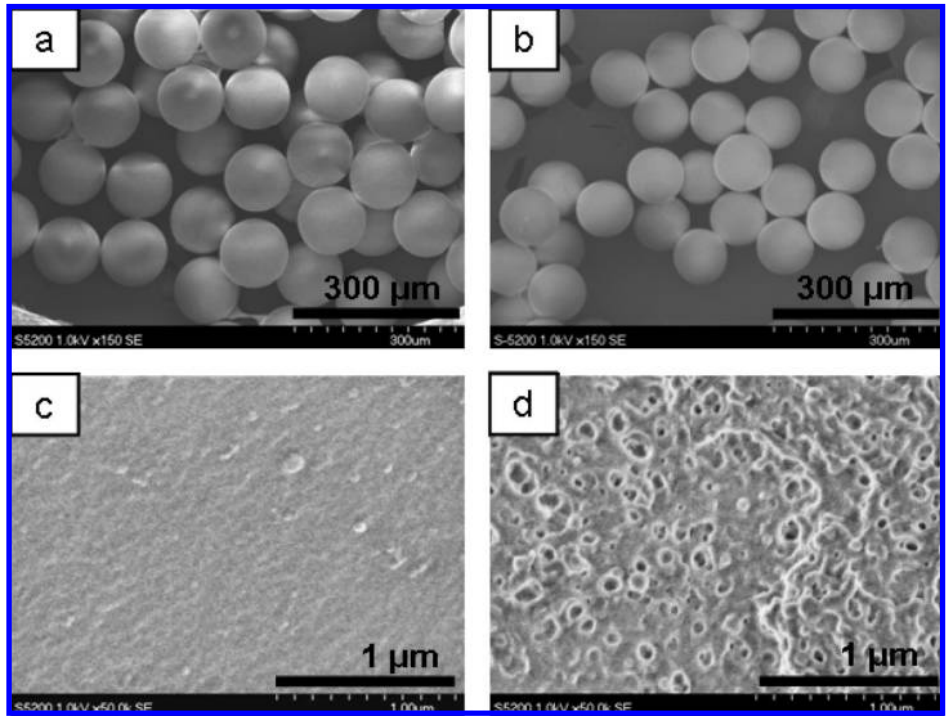

Figure 5. SEM images of the surface of polymer particles synthesized by two-step microfluidic synthesis at $\alpha = 0.98$ (a,c) and $\alpha = 2.29$ (b, d). In order to set the weight ratio α of 0.98 we used $Q_3 = 0.0048$ mL/h and $Q_1 = Q_2 = 0.012$ mL/h. To realize $\alpha = 2.29$, we used $Q_3 = 0.024$ mL/h and $Q_1 = Q_2 = 0.012$ mL/h. The complete compositions of the monomer mixtures supplied to *inlets* 1−3 (see Figure 2) are given in Supporting Information. The flow rates of the 3 wt% aqueous PVA solution introduced in *inlets 4* and *5* were $Q_4 = Q_5 = 1.0$ mL/h (a,c) or $Q_4 = Q_5 = 0.6$ mL/h (b,d), respectively. The UV-irradiation time was 4 min.

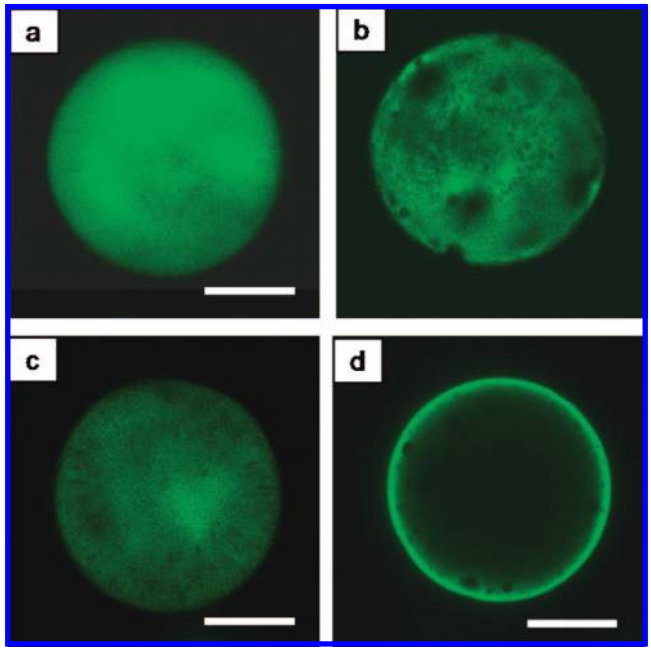

Figure 6. (a,b) Typical confocal microscopy images of polymer particles synthesized by microfluidic synthesis (as in Figure 5) from the TPGDA/PU-pre mixture at $\alpha = 0.98$ (a) and $\alpha = 2.29$ (b). (c,d) Typical confocal microscopy images of particles synthesized by suspension polymerization from the TPGDA/PU-pre mixture at $\alpha = 0.98$ (c) and $\alpha = 2.29$ (d). Excitation wavelength was 488 nm. The focal plane was located at 60 μm below the surface of particles. Scale bar is 50 μm.

polyurethane on the length scales comparable to the resolution of CFM experiments and suggested that no macroscopic phase separation occurred in this system. Figure 6b shows the black domains of the PU-rich phase in the particles synthesized at $\alpha = 2.29$, which indicate substantial—on the micrometer length scale—phase separation between polyTPGDA and polyurethane.

To verify the role of microfluidic synthesis in controlling the morphology of the microbeads, we also synthesized polymer particles using conventional suspension polymerization (see Supporting Information). The droplets produced by microfluidic emulsification of the TPGDA/PU-pre mixtures at $\alpha = 0.98$ and $\alpha = 2.29$ were collected in a vial and exposed to UV-irradiation for 4 min. As expected, the resulting particles featured a broad size distribution, due to the coalescence of the droplets. More importantly, the CFM images of the particles showed that substantial phase separation occurred in both types of microbeads (Figure 6c,d). The signatures of phase separation included the existence of black domains in Figure 6c and a bright rim in the particles synthesized at $\alpha = 2.29$ (Figure 6d), suggesting that a polyTPGDA-rich skin formed on the surface of the microbeads. We ascribe a more homogeneous structure of the particles produced by microfluidic synthesis to a better control of Reaction 1, initiated by the uniform UV-irradiation of every droplet flowing through the microchannel, as well as to more uniform heat dissipation in the continuous aqueous phase.

Conclusions

We have demonstrated the approach to two-step microfluidic polymerization reactions conducted in droplets, in which heat generated in the first free radical polymerization reaction "triggers" the second polycondensation reaction which otherwise occurs at a low rate. Completion of these reactions under optimized conditions led to the continuous microfluidic synthesis of IPN polymer microbeads in the micrometer size range and a narrow polydispersity. These results complement an earlier work on mini-emulsion polymerization of poly(butyl acrylate)/polyurethane of particles in the size range from 90 to 130 nm.[19]

The proposed approach may be useful for other reactions in which the rate constant shows a strong dependence on temperature, however understanding time-dependent heat transfer to the continuous phase is critical in achieving control over the temperature of the reaction mixture compartmentalized in droplets. Second, suppressed phase separation in particles synthesized by microfluidic synthesis may have practical implications in achieving control over the structure of polymer microbeads, however this effect needs further investigation.

Acknowledgment. The authors thank NSERC Canada for funding of this work under Canada Research Chair Grant.

Supporting Information Available: Chemicals and materials, fabrication of microfluidic reactors, methods of characterization of polymers and particle dimensions and structures, and complete ref 2b. This material is available free of charge via the Internet at http://pubs.acs.org.

JA8029174

(19) Nie, Z. H.; Seo, M.; Xu, S. Q.; Lewis, P. C.; Mok, M.; Kumacheva, E.; Garstecki, P.; Whitesides, G. M.; Stone, H. A. *Microfluidics Nanofluidics* **2008**, [Online early access]. doi: DOI 10.1007/s10404−008−0271-y.
(20) Barrère, M.; Landfester, K. *Macromolecules* **2003**, *36*, 5119–5125.